PHYSICAL REVIEW A VOLUME 32, NUMBER 4 OCTOBER 1985

Third-harmonic generation in liquids

F. Kajzar and J. Messier

Commissariat à l'Energie Atomique, Institut de Recherche Technologique et de Developpement Industriel,
Département d'Electronique et d'Instrumentation Nucléaire, Laboratoire d'Etudes et Recherches Avancées,
Centre d'Etudes Nucléaires de Saclay, 91191 Gif-sur-Yvette Cedex, France

(Received 28 December 1984)

Third-order nonlinear susceptibilities of several organic solvents are measured by third-harmonic generation at two laser wavelengths: 1.064 and 1.907 μm. The method used allows a determination of the modulus and phase by interference with the harmonic field generated in the liquid-cell windows. Air contribution to the resulting harmonic intensities is studied in detail. An experimental correction for this effect is proposed and verified for some solvents. Results are discussed within the bond-additivity model.

I. INTRODUCTION

The exact knowledge of the hyperpolarizabilities of organic molecules is important from two points of view: practical (applications in optical devices) and fundamental (testing molecular calculations, bond additivity, nonlinear spectroscopy, interaction with other molecules, etc.). One of the simplest possible methods for its determination is the measure of the harmonic light generated in solution.

The nonlinear susceptibility of liquids has been studied in the past mainly by the static electric-field-induced second-harmonic generation (EFISHG).[1-5] This technique gives directly the total average cubic hyperpolarizability γ ($\equiv \gamma_{XXXX}$ in the laboratory coordinate frame if the applied field direction is collinear with the incident-light polarization vector), which is composed from the following terms:[2,6]

$$\gamma = \gamma^{e} + \gamma^{v} + \gamma^{d} , \tag{1}$$

where γ^e is the purely electronic contribution, γ^v is the vibrational nonlinearity, and γ^d the dipolar contribution (vanishing for centrosymmetric molecules),

$$\gamma^{d} = \frac{\mu\beta}{5kT} , \tag{2}$$

where μ is the dipolar electric moment and β the average second-order susceptibility of molecule.

In the molecular coordinate frame (with the dipole moment μ parallel to the molecular x axis)

$$\beta = \beta_{xxx} + \beta_{xyy} + \beta_{xzz} , \tag{3}$$

and

$$\gamma^{e,v} = \tfrac{1}{5}(\gamma^{e,v}_{xxxx} + \gamma^{e,v}_{yyyy} + \gamma^{e,v}_{zzzz} + 2\gamma^{e,v}_{xxyy} + 2\gamma^{e,v}_{xxzz} + 2\gamma^{e,v}_{yyzz}) . \tag{4}$$

The separation of the corresponding contributions to γ [Eq. (1)] in the EFISHG technique is not evident. Generally γ^d is estimated from the temperature dependence of γ (γ^e and γ^v are assumed to be temperature independent). However, this assumption fails near the electronic or vibronic transitions and/or the two-photon or multiphoton resonances.

The second possibility for separation of the different terms in Eq. (1) is given by the time scale in the response times: γ^e having a response time on the order of 10^{-15} s, whereas γ^v and γ^d are about 2 and 4 orders of magnitude larger, respectively. However, this separation needs the use of a laser with variable pulse length and is difficult in realization and interpretation.

A direct separation of the dipolar term may be obtained by the third-harmonic generation (THG) technique.[7-13] In this technique, because of the random orientation of the dipolar moments, γ^d vanishes. The separation of the electronic and vibrational contributions is also difficult: however, in most cases the first one is dominant, especially near electronic transitions. Other problems arising in this technique are environmental effects, as discussed by Meredith *et al.*[12-14] In fact the laser beam generates the third-harmonic light in surrounding air, which interferes with the harmonic light produced in the measured sample, modifying resulting intensities. This effect, if not eliminated or not taken into account, can lead to large errors in the determination of nonlinear susceptibility.

The present paper deals with THG measurements in liquids by the Maker-fringes technique. This technique allows determination of not only the molecular cubic hyperpolarizability but also its phase. Moreover, the measurements can be done on solutions absorbing at the harmonic frequency (by diminution of the cell thickness). In Sec. II we recall some fundamental equations describing optical wave generation and propagation in isotropic nonlinear media. Section III describes the experimental arrangement and a detailed study of the influence of surrounding sample air on measured intensities for several focal lengths and at two different wavelengths: 1.064 and 1.907 μm. In this section we also give an experimental correction for this effect. In Sec. IV we present some results for several organic solvents at these two wavelengths and we discuss them in Sec. V within the bond-additivity model.

II. THEORY

Optical wave propagation in isotropic nonlinear media has been described by Bloembergen and Pershan[15] and applied for the analysis of Maker fringes from second-harmonic generation by Jerphagnon and Kurtz[16] (see also

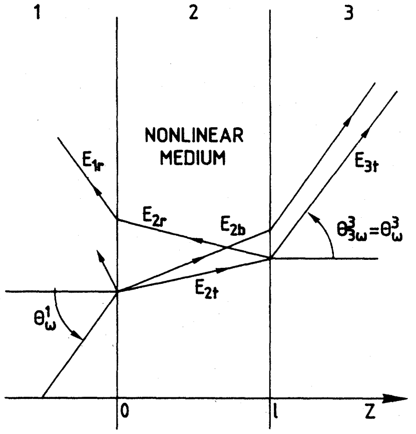

FIG. 1. Harmonic wave propagation in a nonlinear medium immersed between two linear media. Arrows denote wave vectors. The electric fields (only harmonic fields are denoted) as well as the rotation axis are perpendicular to the figure plane.

Kurtz[17]). This formalism has been developed for plane waves. The case of focused laser beams will be discussed below.

Following Bloembergen and Pershan[15] the harmonic electric field created in a nonlinear medium 2 (see Fig. 1) is a sum of bound (b) and two free (t,r) waves (propagating in opposite directions)

$$\begin{aligned} E_2^{3\omega}(\mathbf{r},t) &= E_{2t}^{3\omega}(\mathbf{r})\exp[-i(3\omega t-\mathbf{k}_{3\omega}^{2f}\cdot\mathbf{r})] \\ &\quad + E_{2r}^{3\omega}(\mathbf{r})\exp[-i(3\omega t+\mathbf{k}_{3\omega}^{2f}\cdot\mathbf{r})] \\ &\quad + E_{2b}^{3\omega}(\mathbf{r})\exp[-i(3\omega t-3\mathbf{k}_{\omega}^{2b}\cdot\mathbf{r})]+\text{c.c.}\ , \end{aligned} \tag{5}$$

where the bound wave

$$E_{2b}^{3\omega}(\mathbf{r})=\frac{4\pi P_2^{\mathrm{NL}}}{\Delta\epsilon}\ , \tag{6}$$

with P_2^{NL} the nonlinear polarization created in medium 2 and $\Delta\epsilon=\epsilon_2(\omega)-\epsilon_2(3\omega)$ the dispersion of dielectric constant.

From the boundary conditions for the electric field at the 1-2 and 2-3 interfaces (neglecting reflected waves from interfaces different from that under consideration, see Appendix A), one obtains for harmonic field

$$\begin{aligned} E_2^{3\omega}(l,t) &= \frac{4\pi\chi_2^{(3)}(E^\omega)^3}{\Delta\epsilon}P_2(\theta)e^{i\phi}R(\theta)e^{-i3\omega t} \\ &\quad \times(e^{i(\phi_2^\omega-\phi_2^{3\omega})}-1) \end{aligned} \tag{7}$$

where $\chi_2^{(3)}$ is the third-order nonlinear susceptibility of medium 2

$$\chi_2^{(3)}=N\gamma_2L_\omega^3L_{3\omega}\ , \tag{8}$$

with N the number of molecules in the unit volume and $L_\omega,L_{3\omega}$ the local field factor at fundamental and harmonic frequencies, respectively,

$$L_{\omega,3\omega}=\frac{n^2_{\omega,3\omega}+2}{3}\ . \tag{9}$$

$P_2(\theta)$ (where θ is the incidence angle) is the envelope function arising from the transmission factors between all interfaces and from the boundary conditions between consecutive media (details in Appendix A), ϕ is an overall phase factor, and $\phi_2^\omega(l)$, $\phi_2^{3\omega}(l)$ are phase-mismatch factors in medium 2

$$\phi_2^s(l)=\begin{cases}3k_\omega l\cos\theta_2^\omega, & s=\omega\\ k_{3\omega}l\cos\theta_2^{3\omega}, & s=3\omega\ ,\end{cases}$$

where l is the thickness of medium 2, θ_2^ω and $\theta_2^{3\omega}$ are the propagation angles in medium 2 for fundamental and harmonic waves, respectively, and $R(\theta)$ is the multiple-reflection correction factor (see Appendix B). We note here that the dielectric constants $\epsilon(\omega)$ and $\epsilon(3\omega)$ as well as wave vectors k_ω, $k_{3\omega}$, phase ϕ, $P_2(\theta)$, $R(\theta)$, and propagation angles $\theta_2^\omega,\theta_2^{3\omega}$ may be complex (in an absorbing medium; see Appendix C).

The resulting harmonic field is equal to the sum of contributions from consecutive nonlinear media (5 or 3 in our case, depending whether or not we consider harmonic light from air)

$$E^{3\omega}(\mathbf{r},t)=\sum_j E_j^{3\omega}(\mathbf{r}_j,t)T_j\ , \tag{10}$$

where T_j are the corresponding whole transmission factors and the resulting harmonic light intensity

$$I^{3\omega}=\frac{c\epsilon(3\omega)}{8\pi}\left|\sum_j T_jE_j^{3\omega}(\mathbf{r}_j,t)\right|^2 \tag{11}$$

leads to complex interference patterns (cf. Sec. IV).

For the simplest case of a liquid cell with walls of the same thickness and assuming that the transmission factors for the wall-liquid, liquid-wall interfaces are equal to 1, one obtains a very simple formula for the third-harmonic intensity [see Fig. 2(a)]

$$I^{3\omega}=\frac{256\pi^4T}{c^2}\left|\frac{\chi_L^{(3)}}{\Delta\epsilon_L}\sin\left[\frac{\Delta\phi_L}{2}\right]+\frac{2\chi_G^{(3)}}{\Delta\epsilon_G}\cos\left[\frac{\Delta\phi_L+\Delta\phi_G}{2}\right]\sin\left[\frac{\Delta\phi_G}{2}\right]\right|^2I_\omega^3\ , \tag{12}$$

where subscripts L and G refer to the solvent (solution) and the silica, respectively, and $\Delta\phi_L,\Delta\phi_G$ are phase mismatches in the liquid and glass, respectively,

$$\Delta\phi=\frac{6\pi}{\lambda_\omega}(\epsilon_\omega^{1/2}\cos\theta^\omega-\epsilon_{3\omega}^{1/2}\cos\theta^{3\omega})l\ . \tag{13}$$

In the above, l is the wall (liquid-cell) thickness and θ^ω and $\theta^{3\omega}$ are the propagation angles for fundamental and harmonic waves, respectively, T is an overall transmission factor and I_ω is the fundamental beam intensity.

Formula (12) was derived first by Levine and Bethea[18]

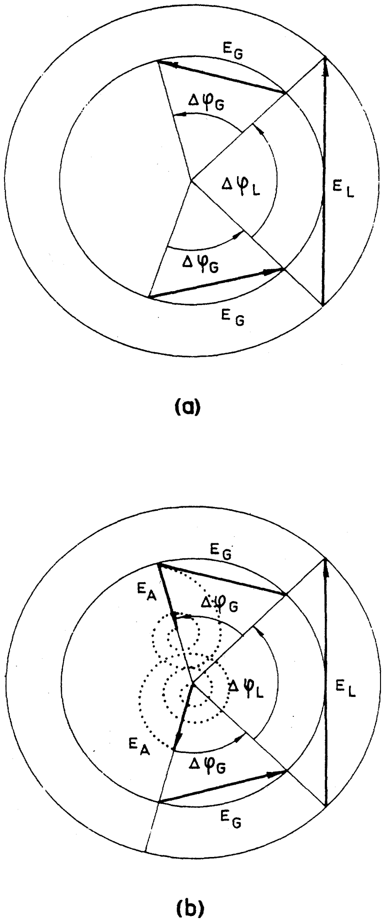

(a)

(b)

FIG. 2. Vibronic diagram without (a) and with (b) air contribution. Subscripts L, G, and A refer to the harmonic fields created in liquid, glass, and air, respectively.

for the second-harmonic generation (SHG) in an electroded cell. However, in their result [Eq. (6)] d should be read as $d/\Delta\epsilon$, which can be important in the case of abnormally dispersed liquids (or solids) and for calibration.

Equation (12) is oversimplified because it completely neglects reflection losses between consecutive nonlinear media (cf. discussion in Ref. 14). It holds only for the cases when the refractive indices of the liquid and glass are the same or very close at both the fundamental and harmonic frequencies as well as when the input and output windows have the same thickness. In a general case the use of this equation can lead to large errors. We quote Eq. (12) because it shows a possibility of a precise determination of the amplitude and phase of one of the nonlinear susceptibilities ($\chi_L^{(3)}$ or $\chi_G^{(3)}$) if the second one ($\chi_G^{(3)}$ or $\chi_L^{(3)}$) as well as $\Delta\epsilon_L$ and $\Delta\epsilon_G$ are known.

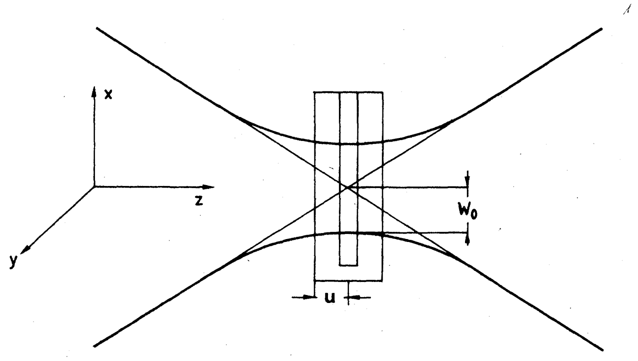

FIG. 3. Liquid-cell arrangement in focused laser beam.

A. Focused laser beams

The above formalism derived for plane waves can also be applied to focused laser beams (in fact a focused laser beam can be considered as a superposition of plane waves). For a thin nonlinear medium, compared to the focal length (we used liquid cells with a thickness of 2—2.5 mm and a focal length of 500 mm), one can assume that the electric field is constant inside the medium and this formalism applies directly. This is no longer true if one considers harmonic light created in surrounding air where the amplitude of electric field changes from one point to another and correspondingly, so does the created harmonic field.

The harmonic light generation for a focused laser beam has been considered by Kleinman *et al.*[19] and applied for THG in gases by Ward and New[20] (see also Boyd and Kleinman[21]). Following these authors for a fundamental Gaussian beam propagating in the z direction

$$E_\omega(\mathbf{r},t)=\frac{E_0}{1+i\tau}\exp[i(k_\omega z-\omega t)] \times\exp\left[-\frac{(x^2+y^2)}{W_0^2(1+i\tau)}\right], \tag{14}$$

where $2W_0$ is the beam waist (see Fig. 3) and

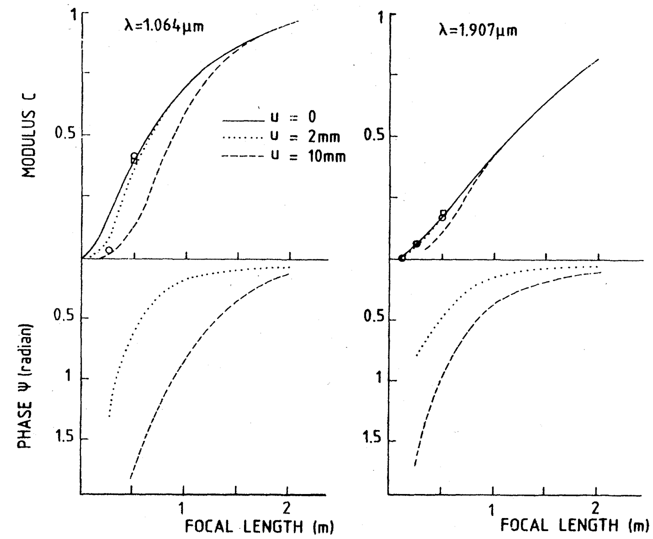

FIG. 4. Calculated modulus C and phase ψ of air contribution at two wavelengths and for different values of u (cf. Fig. 3). Circles and rectangles show measured values of C for a silica plate and liquid cell, respectively.

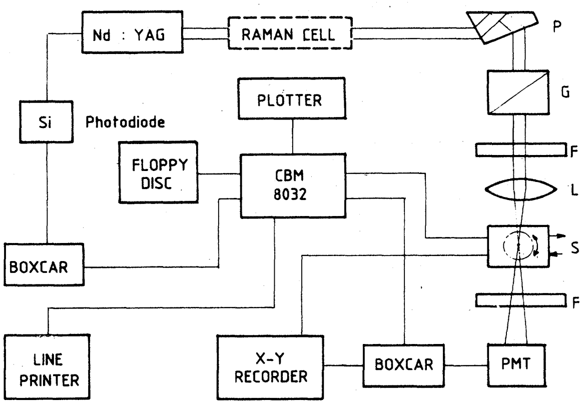

FIG. 5. Schematic representation of experimental arrangement.

$$\tau = \frac{2z}{W_0^2 k_\omega} . \qquad (15)$$

The harmonic field is given by

$$E_{3\omega}(\mathbf{r}) = \frac{4\pi P_A^{\mathrm{NL}} I(u)}{\Delta\epsilon} \exp(ik_{3\omega}z)\exp\left[\frac{-3(x^2+y^2)}{W_0^2(1+i\tau)}\right] , \qquad (16)$$

where the function $I(u)$ is a sum of all contributions from the points between the source (lens) and the point u

$$I(u) = \frac{3\omega}{c}\Delta n \int_{-\infty}^{u} dz' \frac{e^{i\phi}}{(1+i\tau')^2} = Ce^{i\psi} \qquad (17)$$

(cf. Ward and New[20] and Meredith[13]) and Δn is the dispersion in air,

$$\phi = \frac{3\omega}{c}(z'-z)\Delta n \text{ and } \tau' = 2z'/W_0^2 k_\omega .$$

The calculated harmonic contributions for different focal lengths and at two wavelengths are shown in Fig. 4. It is seen that the contribution of air increases with increasing focal length, as expected. This contribution is real at the focus and complex for other points, with an increasing imaginary part going away from the focus.

For an infinite medium $I(\infty)=0$ (see Ward and New[20]). This is no longer true when a rotated sample is placed at focus: this introduces a phase mismatch between air contributions before and after the sample, depending on the rotation angle.

III. EXPERIMENTAL

A schematic representation of the experimental arrangement is shown in Fig. 5. The light source is a 10-pps (pulse per second) Q-switched Nd:YAG laser (where YAG denotes yttrium aluminum garnet) made by Quantel (model YG 481) with pulse duration of about 13 ns and maximum available average energy per pulse of about 850 mJ. A special arrangement (crossed polarizers) enables a continuous variation of the output energy from zero to its maximum value. The sample is rotated and/or translated by stepping motors controlled by a microcomputer Commodore CBM 8032. The eventual variation of fundamental laser power is measured by a rapid Si photodiode and the harmonic light intensity, filtered by a filter assembly, by a photomultiplier tube (PMT): both signals are integrated by boxcar integrators with a very short opening gate time (5 ns for the PMT). The precision in rotation is 0.01° and in translation is 1 μm. The measured harmonic light intensities are stored on floppy disks. The incident light was linearly polarized assuring that the measured quantity was $\chi^{(3)}_{XXXX}$. For the study of the influence of air on the third-harmonic signal a vacuum cell was used with fused silica windows. The vacuum-cell length was adjustable from 12 to 42 cm in order to allow measurements for different focal lengths and to avoid window effects. The sample was placed in the center of the vacuum cell.

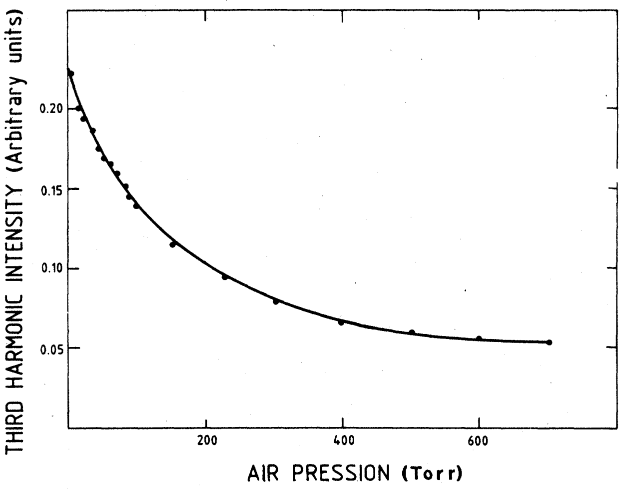

FIG. 6. Third-harmonic intensity variation at 1.064 μm from a silica plate as a function of air pressure.

The THG measurements have been performed at fundamental wavelengths of 1.064 and 1.907 μm, the last obtained by a Raman shift in hydrogen under high pressure (56 bars).

The liquid cells used here were standard commercial cells produced by Hellma and made from Suprasil. The wall thickness was about 1250 μm, whereas the optical pathlength inside the cell was about 1000 μm. The cells were rotated along a vertical axis, parallel to the incident-beam polarization. The sample was carefully oriented in order to align the rotation axis with the laser beam (both being mutually perpendicular). A bad sample orientation is seen in the lack of left- and right-hand symmetry of Maker fringes. A least-squares program permitted a precise determination of the position of the normal to the cell face from the position of interference minima and/or maxima. In addition to the monitoring of fundamental laser power every measurement was calibrated separately by THG on a silica plate or on benzene. All measurements were performed in an air-conditioned room.

IV. EXPERMENTAL RESULTS AND DATA REDUCTION

A. Environmental effects

In Fig. 6 we have shown the measured third-harmonic intensity from a silica plate as a function of air pressure at 1.064 μm and with a focal length of 500 mm. It is seen that the signal decreases quickly with increasing air pressure in the vacuum cell by a factor of about 4 in agreement with the observation by Meredith *et al.*[12,14] This shows evidently that the harmonic field created in air adds oppositely to the harmonic field created in the sample. The same effect is observed with an empty cell or cell filled with a nonlinear liquid. By rotating the sample one varies both harmonic fields created in silica walls and in liquids, whereas the harmonic intensity due to air contribution is angle independent. This is seen in the dependence of the envelope function on the incidence angle (see Fig. 7). The envelope function in air falls more rapidly than in vacuum when the air contribution is smaller than the silica-plate signal and less rapidly for the opposite case.

In order to take this effect into account we have introduced an experimental correction based on the considerations of the preceding section and presented it in Fig. 2(b) (we add harmonic fields created in air before and after the sample with corresponding phases). This gives for the harmonic light intensity the following expression:

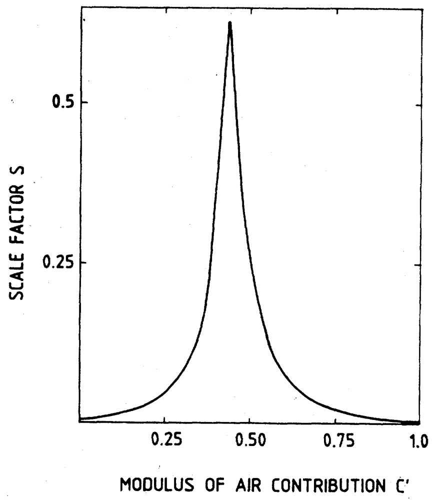

FIG. 8. Scale factor dependence on air contribution parameter C'.

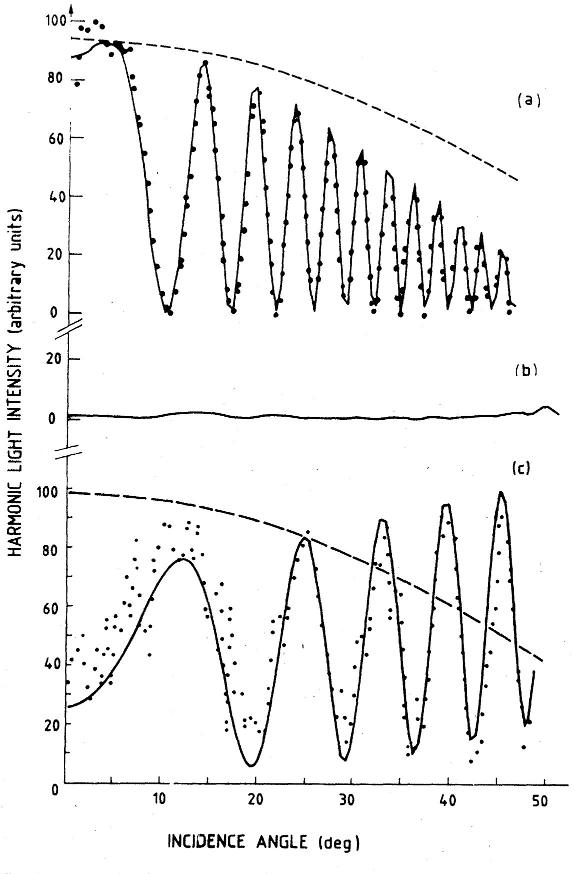

FIG. 7. Calculated (solid line) third-harmonic intensity from a silica plate as a function of incidence angle for following values of air contribution parameter: $C'=0.235$ (a), $C'=0.44$ (b), $C'=0.69$ (c). Points are experimental values for a 1-mm-thick silica plate at 1.064 μm (a) and 1.907 μm (c). Focal length is equal to 50 cm. Broken line shows envelope function in vacuum. Intensities in (a) and (c) are normalized independently to a maximum value whereas in (b) the normalization factor is the same as in (c).

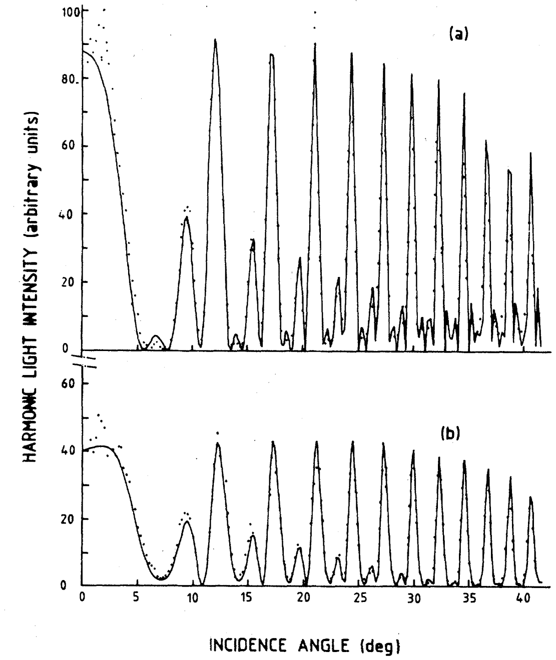

FIG. 9. Calculated and measured third-harmonic intensities from $CHCl_3$ as a function of incidence angle at 1.064 μm in vacuum (a) and in air (b).

$$I^{3\omega} \propto \left| E + C(\chi^{(3)}/\Delta\epsilon)_A \left(T_{3\omega} e^{i(\psi+\theta_1)} - T_{\omega}^3 e^{-i(\psi+\theta_2)}\right) E_{\omega}^3 \right|^2 , \quad (18)$$

where E is the resulting harmonic field created in the cell windows and in the liquid [Eq. (10)], C is the air-contribution parameter, and ψ is its phase [see Eq. (17)]. For a practical convenience we have introduced a new parameter $C' = C(\chi^{(3)}/\Delta\epsilon)_A/(\chi^{(3)}/\Delta\epsilon)_G$ where G and A refer to silica and air, respectively. $T_{3\omega}$ and T_{ω} are transmission factors through the cell at 3ω and ω and θ_1, θ_2 are the phases of the reference free harmonic wave at the cell input and output. In order to determine C' we proceed as follows. First we measure in vacuum the Maker fringes for a silica plate of known thickness. By a least-squares fit of the calculated intensities to the observed ones we determine the refractive-index dispersion of silica and a scale factor S given by

$$S = A \left[\frac{\chi_G^{(3)}}{\Delta\epsilon_G} \right]^2 f(\lambda_{3\omega}) I_{\omega}^3 , \quad (19)$$

where $f(\lambda_{3\omega})$ is the PMT efficiency at the harmonic frequency and A is a factor depending on experimental geometry, filters, and the PMT window transmission

The fit is sensitive up to 10^{-6} on dispersion variation and allows an exact determination of the interference minima and maxima positions. However, the precision in dispersion determination is limited by that in the thickness measurements (in our case $\sim 10^{-3}$). After we introduce air, without changing the silica plate position, and again by a least-squares fit we determine the value of C' (the value of ψ has been found to be close to zero). In Fig. 8 we have plotted, as an example, the scale factor as a function of air contribution parameter C' at 1.064 μm and for a focal length of 500 mm. It is seen that the knowledge of this scale factor allows a precise determination of C' ($C' = 0.235 \pm 0.005$ in this case). In fact there exist two solutions for C' ($C' < 0.44$ and $C' > 0.44$) but there is no ambiguity in the choice of a good value for C' (the envelope of measured intensity as a function of incidence angle falls rapidly in the case of $C' < 0.44$ and increases for $C' > 0.44$, cf. Fig. 7). The fit of interference spectra is quite satisfactory at 1.064 μm [Fig. 7(a)] and worse at 1.907 μm [Fig. 7(c)]. This is due to the experimental difficulty and size of correction. At 1.907 μm the measured signal-to-noise ratio is bad (the silica plate signal is about 30 times weaker than that of benzene). The use of a Raman cell magnifies the laser-intensity fluctuations. The formalism does not take into account the longitudinal mode distribution and fluctuations, the finite-beam-size effects and the influence of surface roughness on harmonic intensity (averaging is better for larger incidence angle because of larger illumination surface). The correction itself is large (the air contribution is significantly larger than the signal itself). We show Fig. 7(c) in order to illustrate the envelope dependence of measured intensity as a function of incidence angle for a large air contribution. This has no impact on our data analysis. At 1.907 μm we used benzene as standard: this one was calibrated with silica in vacuum.

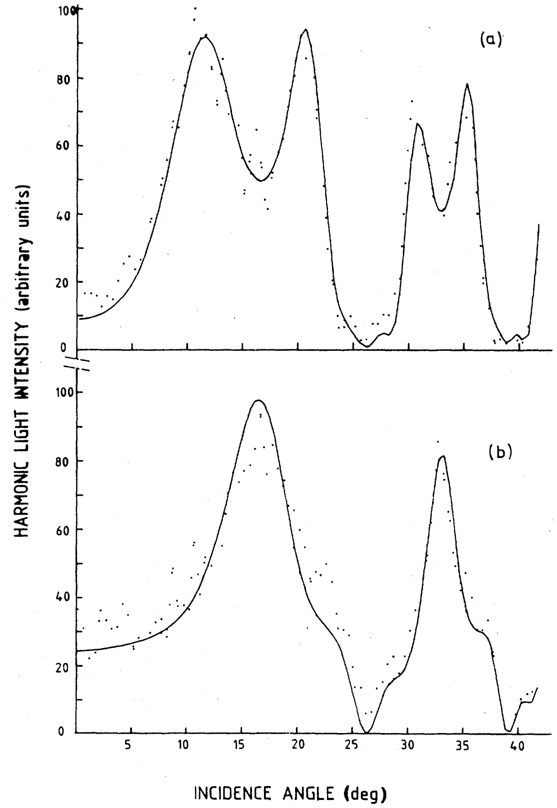

FIG. 10. Calculated and measured third harmonic intensities for $CHCl_3$ as a function of incidence angle at 1.907 μm in vacuum (a) and in air (b).

The measurements have been performed at different focal lengths and the results for C' are presented in Fig. 4 while some characteristic fringe patterns, in air and in vacuum, are shown in Figs. 9 and 10. As expected (see Fig. 4) the values of C' are negligible at focal lengths smaller than 15 cm at 1.064 μm and smaller than 10 cm at 1.907 μm.

Taking for air[22] and silica[23] the following values,

$$(\Delta n)_A = 1.085 \times 10^{-5}, \quad (\Delta n)_G = 2.65 \times 10^{-2}, \quad (\chi^{(3)})_G = 3.11 \times 10^{-14} \text{ esu } (\lambda = 1.064\ \mu\text{m})$$

$$(\Delta n)_A = 3 \times 10^{-6}, \quad (\Delta n)_G = 1.745 \times 10^{-2}, \quad (\chi^{(3)})_G = 2.79 \times 10^{-14} \text{ esu } (\lambda = 1.907\ \mu\text{m}) ,$$

it would be possible, in principle, from the definition of C' to deduce the cubic susceptibility of air. We find

$$(\chi_{XXXX}^{(3)})_A = 7.0 \times 10^{-18} \text{ esu } \quad (\lambda = 1.064\ \mu\text{m}) ,$$

$$(\chi_{XXXX}^{(3)})_A = 1.8 \times 10^{-17} \text{ esu } \quad (\lambda = 1.907\ \mu\text{m}) .$$

These numbers are larger than those reported in literature: $(\chi_{XXXX}^{(3)})_A = 1.6 \times 10^{-18}$ esu (Ref. 24) and 4.7×10^{-18} esu (Ref. 20). Owing to several approximations we used in the interpretation of experimental data (Gaussian beam, single mode laser), the determination of C' does not permit a

TABLE I. Nonlinear cubic susceptibilities and coherence lengths obtained from the least-squares fit of Eq. (11) to experimental data for suited solvents at 1.907 μm. The estimated error in nonlinear susceptibilities is of ±5% (the relative precision between solvents is better) and in coherence length of ±2%. The refractive indices at 1.907 μm are combined data from Landolt-Börnstein tables (Ref. 27) and from Ref. 28. The absolute values of $\chi^{(3)}$ and γ are calculated using for silica $\chi^{(3)}=2.79\times10^{-14}$ esu (Ref. 12). For absorbing solvents the temperature of measurements corresponds to an equilibrium temperature which may be higher than 20 °C.

Solvent	Chemical formula	n_ω	$\kappa_\omega\times10^5$	Coherence length in μm	$\chi^{(3)}_{\rm sol}/\chi^{(3)}_{\rm SiO_2}$	$\chi^{(3)}$ (10^{-14} esu)	$\gamma/\gamma_{\rm SiO_2}$	γ (10^{-36} esu)	γ (10^{-36} esu) other studies
Benzene	C_6H_6	1.480 08	1.0	17.25	3.81	10.64	1.089	4.07	3.85[a]
Carbon tetrachloride	CCl_4	1.443 80	0.0	28.74	2.64	7.37	0.900	3.36	3.09[b]
Chloroform	$CHCl_3$	1.434 92	0.0	30.39	2.05	5.72	0.608	2.27	2.29[b]
Dichloromethane	CH_2Cl_2	1.4232	0.4	33.96	1.71	4.77	0.417	1.55	
Cyclohexane	C_6H_{12}	1.442 68	2.9	33.42	2.32	5.60	0.809	3.02	
N-hexane	$CH_3(CH_2)_4CH_3$	1.3645	2.4	38.73	1.91	5.33	1.115	4.17	
Acetone	CH_3COCH_3	1.350 56	2.0	36.36	1.47	4.10	0.504	1.88	
Methanol	CH_3OH	1.315 58	2.8	24.99	1.12	3.12	0.233	0.87	0.80[a]
Ethanol	C_2H_5OH	1.334 31	2.8	27.10	1.48	4.13	0.399	1.49	1.33[a]
Dimethylformamide	$HCON(CH_3)_2$	1.414 52	2.1	22.41	1.81	5.05	0.546	2.03	
Nitrobenzene	$C_6H_5NO_2$	1.520 69	1.4	12.76	6.02	16.8	1.758	6.57	5.37[a]
Pyridine	C_5H_5N	1.488 59	1.3	18.40	3.60	10.04	0.926	3.46	3.36[a]
Fused silica	SiO_2	1.439 53	0.0	18.24	1	2.79[b]	1	3.73	

[a] Reference 13.

[b] Reference 12.

precise measurement of $\chi^{(3)}$, but is just a way to take into account experimentally the air contribution. Nevertheless this shows how the calibration of harmonic intensities with respect to a single plate or cell windows in air can lead to large errors.

B. Nonlinear susceptibility of organic solvents

In the most general case of measurements in air there are five nonlinear regions (this number reduces to three in the case of measurements in vacuum) and the number of free parameters is equal to 11 (refractive indices of silica and of solvent at fundamental and harmonic frequencies, C' and ψ for air, $\chi^{(3)}$ and its phase for liquid, thickness of silica walls, and thickness of liquid). In reality the number of free parameters may be limited to three: dispersion, the nonlinear susceptibility of the liquid, and its phase. The other ones can be determined and/or measured independently. In practice we have proceeded as follows: first we have measured harmonic intensities generated in an empty liquid cell, measuring thickness of walls and of the compartment for liquid. As for silica plate the measurements have been done in air and in vacuum and the observed intensities fitted using Eq. (18) as described before with all parameters for liquid cell and for air kept constant. All studied solvents are transparent at 1.064 μm and at harmonic frequencies, but some of them absorb slightly at 1.907 μm. In Table I we give the imaginary parts of refractive indices κ_ω for studied solvents measured from transmission in a 1-cm-thick liquid cell. These are very small ($\kappa_\omega \sim 10^{-5}$ or less) and as discussed in Appendix C, the harmonic light generation in this case can be considered, as in a nonabsorbing medium, to have complex transmission factors and factors arising from boundary conditions, as well as ϵ complex and phase mismatches ϕ,ϕ_2^ω ($\phi_2^{3\omega}$ if absorption at harmonic frequency) [see Eqs. (7), (11), (18), and (A5)—(A8)]. This is achieved by replacing refractive indices in corresponding formulas by the complex ones. The absorption (at fundamental and/or harmonic frequency) introduces an additional phase shift, which may be confused with the phase of $\chi^{(3)}$ if not taken into account correctly. This additional phase shift is negligible in our case (see Appendix C) and was neglected in data analysis. Thus in the fitting procedure we have varied only the modulus of nonlinear susceptibility, its phase as well as dispersion, neglecting the phase arising from absorption at fundamental frequency (see Appendix C). The absorption at fundamental frequency was taken into account by introducing the complex refractive index with κ_ω values given in Table I.

First, we have observed that the air contribution parameter C' for liquid cell and for silica plate, within experimental accuracy, were close to one another at a given wavelength and focal length. For three solvents benzene, chloroform, and dimethylformamide (DMF) we have done THG measurements in vacuum and in air, verifying that the value of parameter C' determined for an empty cell holds also well for filled cell. The calculated values for these three solvents in vacuum and in air at both

TABLE II. Cubic nonlinearities (in silica hyperpolarizability units) measured in air and in vacuum for three solvents. The air-contribution coefficient C' is equal to 0.225 and 0.66 at 1.064 and 1.907 μm, respectively, and the focal length is 500 mm. The estimated error in the χ ratios is $\pm 5\%$.

	$\lambda_\omega = 1.064$ μm		$\lambda_\omega = 1.907$ μm	
Solvent	$\chi^{(3)}_{\text{sol}}/\chi^{(3)}_{\text{SiO}_2}$ in vacuum	$\chi^{(3)}_{\text{sol}}/\chi^{(3)}_{\text{SiO}_2}$ in air	$\chi^{(3)}_{\text{sol}}/\chi^{(3)}_{\text{SiO}_2}$ in vacuum	$\chi^{(3)}_{\text{sol}}/\chi^{(3)}_{\text{SiO}_2}$ in air
Benzene	3.83	3.85	3.81	3.86
Chloroform	2.20	2.26	2.05	2.10
Dimethylformamide	1.79	1.85	1.91	1.81

wavelengths are given in Table II.

At 1.064 μm ($C' < 0.44$) the interference patterns in air and in vacuum are similar (see Fig. 9) whereas at 1.907 μm ($C' > 0.44$) they are quite different (see Fig. 10). This is due to the fact that in the last case the air contribution is more important than that of silica and the difference between them adds to the harmonic field created in solvent.

The liquid cell was cleaned *in situ* and measurements repeated for other solvents in air. Very good reproducibility of interference patterns was conserved during the measurements. The results of least-squares fit for all studied solvents, together with available literature data at 1.064 and 1.907 μm are given in Tables III and I, respectively. Generally a good agreement is seen with the results of Meredith *et al.*[12,13] at 1.907 μm. At 1.064 μm there are no THG measurements for these solvents. The results given in Table III were obtained by electric-field-induced second-harmonic generation. Except benzene, which is a nonpolar solvent, all γ are higher than ours. This probably is due to the difficulty in the separation of dipolar parts in γ [see Eqs. (1) and (2)]. The values of $\chi^{(3)}_{XXXX}$ [and subsequently the values of γ_{XXXX} obtained through Eq. (8)] were calculated using for silica $\chi^{(3)}_{XXXX} = 2.79 \times 10^{-14}$ esu as determined by Meredith *et al.*[12] at 1.907 μm (the same value was reported by Levenson[25] from the three-wave-mixing experiment). There is no corresponding value at 1.064 μm. From the Miller's rule $\chi^{(3)} \sim (\chi^{(1)})^4$ and from refractive index dispersion[23] one obtains at 1.064 μm $\chi^{(3)}_{XXXX} = 3.11 \times 10^{-14}$ esu which we used to calibrate the nonlinear susceptibilities at this wavelength. Anyway the values for $\chi^{(3)}$ and γ given in Tables I and III can be easily recalibrated to those of silica or of one of the studied solvents with better-known values.

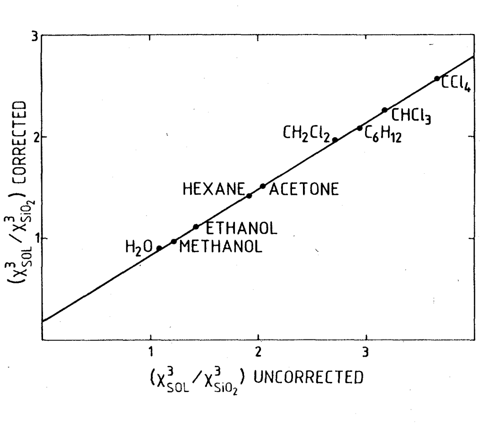

FIG. 11. $\chi^{(3)}_{\text{sol}}/\chi^{(3)}_{\text{SiO}_2}$ corrected vs uncorrected for air contribution ratio. Solid line shows a least-squares fit as described in text.

We have found, within experimental accuracy, zeroth phases for the nonlinear susceptibilities of studied liquids at both wavelengths.

Other elements of cubic tensor for these solvents can be obtained from the symmetry conditions (see Buckingham and Orr[26])

$$\gamma_{iikk} = \tfrac{1}{3}\gamma_{XXXX}, \quad i,k \text{ all permutation of } X,Y,Z$$

$$\gamma_{iiii} = \gamma_{xxxx}, \quad i = Z,Y \; .$$

In Fig. 11 we compare the ratios of liquid nonlinear susceptibilities to those of fused silica corrected and uncorrected for air contribution for several organic solvents measured at 1.064 μm. It is seen that the uncorrected values are larger than the corrected ones in agreement with our preceding discussion on influence of air, and all points lie on the same line. A least-squares fit gives the following relation between corrected and uncorrected values

$$(\chi^{(3)}_{\text{sol}}/\chi^{(3)}_{\text{SiO}_2})_{\text{corr}} = 0.653(\chi^{(3)}_{\text{sol}}/\chi^{(3)}_{\text{SiO}_2})_{\text{uncorr}} + 0.183 \; .$$

The intercept 0.183 is close to the correction for air (0.225) (it should be air contribution factor, C', if one neglects all transmission factors).

V. DISCUSSION

A. Bond hyperpolarizabilities

From Eq. (4) it follows that the average molecular third-order susceptibility is a scalar quantity. Thus the data from Tables I and III should allow a determination of bond hyperpolarizabilities within the bond additivity model.[26] The simplest cases are those of H_2O and of CCl_4 which yield the values of O-H and C-Cl hyperpolarizabilities with a good precision. For the O—H bond we obtain $\gamma_{\text{O-H}} = (0.42 \pm 0.02) \times 10^{-36}$ esu at 1.064 μm (because of absorption of water at 1.907 μm similar determination was not possible). For determination of hyperpolarizability of C—Cl and C—H bonds we have used a series of three solvents: CCl_4, $CHCl_3$, and CH_2Cl_2 and the values for C—Cl and C—H bonds were obtained by a least-squares method. The results of such fits are given in Table IV for

TABLE III. Nonlinear cubic susceptibilities and coherence lengths obtained from the least-squares fit of Eq. (11) to experimental data for studied organic solvents of 1.064 μm. The estimated error in nonlinear susceptibilities is ±5% whereas the error in coherence length is ±2%. The refractive indices at 1.064 μm are combined data from the Landolt-Börnstein tables (Ref. 27) and from Ref. 28. The absolute values of $\chi^{(3)}$ and γ are calculated using $\chi^{(3)}=3.11\times10^{-14}$ esu (for silica).

Solvent	Chemical formula	n_ω	Coherence length in μm	$\chi^{(3)}_{\mathrm{sol}}/\chi^{(3)}_{\mathrm{SiO_2}}$	$\chi^{(3)}$ (10^{-14} esu)	$\gamma/\gamma_{\mathrm{SiO_2}}$	γ (10^{-36} esu)	γ (10^{-36} esu) other studies
Benzene	C_6H_6	1.48258	2.64	3.85[a]	11.98	1.095	4.40	3.40±0.34[c]
Carbon tetrachloride	CCl_4	1.44678	4.85	2.56	7.96	0.904	3.63	
Chloroform	$CHCl_3$	1.43783	5.20	2.25[a]	7.00	0.674	2.71	2.80±0.28[c]
Dichloromethane	CH_2Cl_2	1.42862	5.61	1.97	6.13	0.482	1.94	
Cyclohexane	C_6H_{12}	1.44318	5.94	2.08	6.47	0.826	3.32	
N-hexane	$CH_3(CH_2)_4CH_3$	1.36500	7.22	1.42	4.42	0.852	3.43	
Acetone	CH_3COCH_3	1.35347	6.86	1.51	4.69	0.449	1.80	2.70±0.27[c]
Methanol	CH_3OH	1.32000	8.41	0.96	2.98	0.207	0.83	0.86[d]
Ethanol	C_2H_5OH	1.33989	7.74	1.11	3.45	0.315	1.27	2.10±0.21[c]
Dimethylformamide	$HCON(CH_3)_2$	1.41500	4.43	1.79[a]	5.57	0.549	2.20	4.34[e]
Water	H_2O	1.32612	7.40	0.90	2.80	0.208	0.83	1.44[d]
Fused silica	SiO_2	1.44967	6.63	1	3.11[b]	1	4.02	

[a] Measured in vacuum.

[b] Calculated from Miller's rule using $\chi^{(3)}=2.79\times10^{-14}$ esu determined by Meredith *et al.* (Ref. 12) at 1.907 μm.

[c] EFISHG at 1.064 μm (Ref. 2).

[d] EFISHG at 1.064 μm (Ref. 3).

[e] EFISHG at 1.064 μm (Ref. 5).

both wavelengths and compared with those obtained by Meredith *et al.*[13] Our data confirm the negative value of C-H hyperpolarizability observed by Meredith *et al.*[13] at 1.907 μm. The corresponding value at 1.064 μm is small and positive. This variation of $\gamma_{\mathrm{C-H}}$ can be understood by the influence of a large C-H stretching vibration at about 3.3 μm. Contrariwise, for C—Cl bond, which is a saturated bond, we observe the same values of γ at both wavelengths. Other bond cubic susceptibilities given in Table IV at 1.064 μm are obtained by using the values of $\gamma_{\mathrm{C-H}}$ and $\gamma_{\mathrm{O-H}}$ determined as described above. The uncertainty in these values are much larger because they accumulate all uncertainties of preceding determinations. A least-squares fit for all studied solvents gives unreasonable results. This is probably not only due to the experimental inaccuracy, but also to the validity of the additivity model and universality of the local field correction [Eq. (9)] calculated for a spherical molecule. For example using the values for $\gamma_{\mathrm{C-H}}$ and $\gamma_{\mathrm{C-C}}$ from Table IV one obtains too a low value of γ for larger and flat molecules like hexane and cyclohexane.

B. Dispersion of cubic hyperpolarizabilities

The precision in the third-order nonlinear susceptibility values, given in Tables I and III at 1.907 and 1.064 μm, respectively, does not allow a strict determination of their dispersion. It allows, however, to observe some tendencies and regularities for particular solvents. As we mentioned before, the constancy in CCl_4 hyperpolarizability and its systematic decrease at 1.907 μm with increasing number of C—H bonds for other solvents from the same family ($CHCl_3$, CH_2Cl_2) can be well understood by frequency behavior of $\gamma_{\mathrm{C-Cl}}$ and $\gamma_{\mathrm{C-H}}$. For other solvents like benzene, DMF, and acteone we observe nearly the same dispersion in $\chi^{(3)}$ between 1.907 and 1.064 μm as that of fused silica. The solvents with the largest absorption at 1.907 μm also have a larger $\chi^{(3)}$ value at this wavelength. This may be due to a significant Raman contribution. In any case this increase in the $\chi^{(3)}$ value cannot be due to a local heating caused by light absorption. The refractive index variation dn/dT is negative for studied solvents[27]

TABLE IV. Average bond hyperpolarizabilities calculated within bond-additivity model as described in text.

Bond	γ(10^{-36} esu) $\lambda=1.064$ μm	$\lambda=1.907$ μm	
C—Cl	0.90±0.04[a]	0.83±0.04[a]	0.7725[b]
C—H	0.05±0.04[a]	−0.10±0.04[a]	−0.0275[b]
O—H	0.42±0.02[c]		0.5531[b]
C—C	0.32±0.42		0.6211[b]
C=C	1.03±1.52		0.61[b]
C—O	0.24±0.19		0.30[b]
C=O	0.82±1.10		0.99[b]

[a] Least-squares fit values for three solvents: CCl_4, $CHCl_3$, CH_2Cl_2.

[b] Reference 13.

[c] Calculated from cubic susceptibility of water.

and according to Miller's rule a local temperature increase will result in a decrease of $\chi^{(3)}$.

VI. CONCLUSION

The advantages of the THG technique for molecular hyperpolarizability determinations have been largely discussed by Meredith *et al.*[12,13] The technique, used by these authors, is well adapted for the determination of nonlinear susceptibilities of a pure, nonabsorbing liquid because it employs thick liquid cells. In our case, as we intend further to study absorbing liquids, we developed a method which can be used for very thin cells. The measurements are weakly sensitive to the surface flatness, the laser beam being focused on a small area which varies slowly with incident angle. The commercial liquid cells used by us have a sufficient quality in order to satisfy the requirement of surface flatness.

By fitting the resulting harmonic light intensities generated in the liquid and glass one can determine not only the absolute value of nonlinear susceptibility but also its phase, and simultaneously the dispersion of refractive index.

The results presented in Sec. IV show the importance of environmental effects. The harmonic fields generated in air before and after the sample lead to a decrease of the measured intensities. The magnitude of this effect increases with focal length and depends also on the laser wavelength. The proposed correction allows us to take it into account, if for some reason it is impossible to work in vacuum.

The results for $\chi^{(3)}$ at 1.064 and 1.907 μm show that the bond additivity model gives coherent results for a series of homologous solvents (CCl_4, $CHCl_3$, CH_2Cl_2). Problems appear when one wants to extend this model for a larger number of different molecules.

For the three molecules cited above we observe a slight decrease of γ between 1.064 and 1.907 μm which may be due to the negative contribution of the C-H stretching vibration in near infrared.

APPENDIX A: THIRD-HARMONIC GENERATION IN A NONLINEAR SLAB

For the sake of simplicity we consider first a nonlinear medium 2 immersed between two linear media 1 and 3 (see Fig. 1) and we limit ourselves to an incident transverse electric wave. There are the following waves propagating in these media to be considered:

$$E_{1r}e^{-i3\omega(t+N^1_{3\omega}z/c)} \tag{A1a}$$

(free wave transmitted from 2 to 1),

$$E_{2t}e^{-i3\omega(t-N^2_{3\omega}z/c)} \tag{A1b}$$

(free wave propagating in 2),

$$E_{2r}e^{-i3\omega(t+N^2_{3\omega}z/c)} \tag{A1c}$$

(free wave reflected at 2-3 interface),

$$E_{3t}e^{-i3\omega[t-N^3_{3\omega}(z-l)/c]} \tag{A1d}$$

(free wave transmitted to 3),

$$E_{2b}e^{-i3\omega(t-N^2_{\omega}z/c)} \tag{A1e}$$

(bound wave propagating in 2), with

$$N^j_{\omega,3\omega}=n^j_{\omega,3\omega}\cos\theta^j_{\omega,3\omega} , \tag{A2}$$

where $n^j_{\omega,3\omega}$ is the refractive index (in general complex) of medium j at frequency ω (3ω) and $\theta^j_{\omega,3\omega}$ propagation angles for bound (harmonic) waves in medium j.

The boundary conditions for the electric and magnetic fields at the 1-2 ($z=0$) and 2-3 ($z=l$) interfaces give the following sets of linear equations:

For $z=0$

$$\begin{gathered} z_{1r}=E_{2t}+E_{2r}+E_{2b} , \\ -N^1_{3\omega}E_{1r}=N^2_{3\omega}(E_{2t}-E_{2r})+N^2_{\omega}E_{2b} . \end{gathered} \tag{A3}$$

For $z=l$

$$\begin{gathered} E_{2t}e^{i\phi_3}+E_{2r}e^{-i\phi_3}+E_{2b}e^{i\phi_1}=E_{3t} , \\ N^2_{3\omega}(E_{2t}e^{i\phi_3}-E_{2r}e^{-i\phi_3})+N^2_{\omega}E_{2b}e^{i\phi_1}=N^3_{3\omega}E_{3t} , \\ \phi_m=3\omega N^2_{m\omega}l/c \quad (m=1,3) . \end{gathered} \tag{A4}$$

By solving simultaneously these two sets of equations and using Eq. (6) for the bound wave, one obtains for the harmonic wave in medium 3

$$\begin{aligned} E_{3t}=&\frac{4\pi P^{\mathrm{NL}}e^{i3\omega lN^2_{3\omega}/c}}{\epsilon_2(\omega)-\epsilon_2(3\omega)} \\ &\times(A_1\{\exp[i3\omega l(N^2_{\omega}-N^2_{3\omega})/c]-1\} \\ &+A_2\{\exp[i3\omega l(N^2_{\omega}+N^2_{3\omega})/c]-1\})A_3^{-1} , \end{aligned} \tag{A5}$$

where

$$A_1=\frac{N^2_{3\omega}+N^2_{\omega}}{N^3_{3\omega}+N^2_{3\omega}} , \tag{A6}$$

$$A_2=\left[\frac{N^2_{3\omega}-N^2_{\omega}}{N^3_{3\omega}+N^2_{3\omega}}\right]\left[\frac{N^1_{3\omega}-N^2_{3\omega}}{N^1_{3\omega}+N^2_{3\omega}}\right] , \tag{A7}$$

$$A_3=1-\left[\frac{N^1_{3\omega}-N^2_{3\omega}}{N^1_{3\omega}+N^2_{3\omega}}\right]\left[\frac{N^3_{3\omega}-N^2_{3\omega}}{N^3_{3\omega}+N^2_{3\omega}}\right]e^{i6\omega N^2_{3\omega}l/c} . \tag{A8}$$

The coefficient A_2 is small and the second term in Eq. (A5) can be neglected. In practice, this corresponds to neglectings in the boundary conditions all reflected waves from interfaces other than those under consideration. This condition is fulfilled for thick nonlinear media, as in our case. Thus Eq. (A5) reduces to Eq. (7) and the resultant harmonic field coming from several nonlinear media is given by a sum of harmonic fields generated in successive media [Eq. (10)] multiplied by corresponding transmission factors.

The problem can be treated rigorously by solving a system of $2(n-1)$ equations (boundary conditions) on $2(n-1)$ variables (amplitudes of electric free waves) where n is the number of nonlinear media.

APPENDIX B: MULTIPLE REFLECTIONS

The above formalism takes account of all reflections of harmonic waves but neglects those of the fundamental one. For the sake of simplicity we consider a nonlinear plate. The case of a liquid cell can be well approximated by a slab with thickness l equal to the sum of the liquid-compartment and the window thicknesses. In fact because of the small difference of refractive index between fused silica and most of the organic liquids, reflections on these interfaces are also small. In our case only reflections at silica-vacuum and vacuum-silica interfaces [$r=(n-1)/(n+1)\simeq 0.18$ at 1.06 μm] are important.

The fundamental field inside a parallel plate with thickness l can be described by two waves, a forward E_ω^i and a backward E_ω^r given by

$$E_\omega^i = E_{2t}^\omega \frac{1}{1-r^2 e^{i2\phi}} e^{i(k_i' z\cos\theta' - \omega t)} , \tag{B1}$$

$$E_\omega^r = E_{2t}^\omega \frac{r e^{i2\phi}}{1-r^2 e^{i2\phi}} e^{i(k_r' z\cos\theta' + \omega t)} , \tag{B2}$$

where $\phi=(2\pi l/\lambda)n\cos\theta'$ (θ' is the propagation angle inside the plate). E_{2t}^ω is the amplitude of the incident wave in the plate, without multiple reflections.

The interaction between E_ω^i and E_ω^r gives rise to four bound waves and eight free waves inside the nonlinear medium and to eight free waves outside (see Table V). The phase factor $e^{2i\phi}$ introduces rapid oscillations of the field amplitude with the angle of incidence, with a period $\Delta\theta$ given by

$$\Delta\theta=\lambda(n^2-\sin^2\theta)^{3/2}/nl\sin^2\theta . \tag{B3}$$

For a silica plate with $l=1000$ μm and $\theta=5°$ we obtain at 1.064 μm, $\Delta\theta=0.7°$, and a value 3.5 times smaller for our liquid cell. It means that on the overall interference spectra will be superposed (outside normal incidence) a rapidly oscillating component due to multiple reflections. Because of the laser-beam divergence and large PMT window diameter, the resolution will be not sufficient in order to observe these oscillations, and we will observe an average modification of the harmonic intensity given by a correction factor

$$R(\theta)=\langle\, |(1+r^2e^{i2\phi})^3|^2\rangle_{\text{av}}=1+9r^4+O(r^6) , \tag{B4}$$

which is equal to 1.009 outside the normal incidence.

TABLE V. Bound waves due to multiple reflections in a plane parallel slab.

Bound wave $\frac{4\pi}{(\Delta\epsilon)}\chi^{(3)}(E_\omega^\alpha E_\omega^\beta E_\omega^\gamma)$ $\alpha,\beta,\gamma=i$ or r	Relative amplitude of the bound waves normalized to E_{2b} [Eqs. (A1)]
$E_\omega^i E_\omega^i E_\omega^i$	$(1+r^2e^{2i\phi})^3$ $\neq 1+3r^2e^{6i\phi}$
$E_\omega^i E_\omega^i E_\omega^r$	$re^{i\phi}$
$E_\omega^i E_\omega^i E_\omega^r$	$r^2e^{4i\phi}$
$E_\omega^r E_\omega^r E_\omega^r$	$r^3e^{6i\phi}$

All these considerations show that the multiple reflections are cumbersome and negligible except at normal incidence. Some anomalies observed in our interference spectra near normal incidence (see Figs. 7, 9, and 10) may be due to these effects.

The preceding analysis supposes that the fields E_ω^i and E_ω^r are coherent. For reasons like surface roughness, thickness variation, finite beam size, and laser-mode fluctuations this coherence may be lost. This loss of coherence will take place, for instance, when the thickness variation

$$\Delta l > \lambda/8n_\omega = \begin{cases} 0.09\ \mu\text{m} & \text{at } \lambda=1.064\ \mu\text{m} \\ 0.16\ \mu\text{m} & \text{at } \lambda=1.907\ \mu\text{m}, \end{cases}$$

whereas the Maker fringes are observed for

$$\Delta l \le \lambda/12(n_{3\omega}-n_\omega) = \begin{cases} 3.3\ \mu\text{m} & \text{at } \lambda=1.064\ \mu\text{m} \\ 9.1\ \mu\text{m} & \text{at } \lambda=1.907\ \mu\text{m}. \end{cases}$$

Thus experimentally we are probably closer to the second case (incoherent reflected beams) than to the first (coherent reflections). In the second case the multiple correction will still be much smaller, being proportional to r^m ($m=6$ or 12).

APPENDIX C: THIRD-HARMONIC GENERATION IN AN ABSORBING MEDIUM

The second-harmonic generation in an absorbing medium was considered by Chemla and Kupecek.[29] A generalization to the third-harmonic generation case is straightforward.

Consider an absorbing medium with a complex refractive index

$$n=n_r+i\kappa . \tag{C1}$$

Snell's law, $n\sin\theta=\text{const}$, implies that in an absorbing medium the propagation angle θ' is also complex

$$\theta'=\theta_r+i\theta_i . \tag{C2}$$

Setting

$$n\cos\theta'=n_r\left[\cos\theta_r+\frac{i\kappa}{n_r\cos\theta_r}\right] , \tag{C3}$$

one obtains the following equation in $\cos^2\theta_r$:

$$n_r^2\cos^4\theta_r-(n_r^2-\kappa^2-\sin^2\theta)\cos^2\theta_r-\kappa^2=0 , \tag{C4}$$

where θ is the incidence angle (in a transparent medium). The solutions of Eq. (C4) are always real. In a slightly absorbing medium ($\kappa \ll 1$) one gets

$$\cos^2\theta_r=1-\frac{\sin^2\theta}{n_r^2}+\frac{\kappa^2}{2}\left[1-\frac{\cos^2\theta}{n_r^2}\right]+O(\kappa^4) . \tag{C5}$$

It means that in this limit the refracted wave can be considered as propagating in a transparent medium with an exponential decrease of amplitude

$$\exp(ikz)=\exp(iz\omega n_r \cos\theta_r/c - z\omega\kappa/c\,\cos\theta_r)\ . \qquad \text{(C6)}$$

For liquids absorbing at the fundamental and/or at the harmonic frequency the corresponding mismatch factors in Eq. (7) will be given by

$$\phi_2^{\omega}(l)=3\omega l(n_\omega \cos\theta_2^{\omega}+i\kappa_\omega/\cos\theta_2^{\omega})/c\ ,$$
$$\phi_2^{3\omega}(l)=3\omega l(n_{3\omega}\cos\theta_2^{3\omega}+i\kappa_{3\omega}/\cos\theta_2^{3\omega})/c\ . \qquad \text{(C7)}$$

At the output of an absorbing medium with thickness l the amplitude of the fundamental wave will be diminished by a factor of

$$E^{\omega}(l)=E^{\omega}(0)\exp(-\kappa_\omega \omega l/c\,\cos\theta_2^{\omega})\ , \qquad \text{(C9)}$$

and this value has to be used in Eq. (7) at the input of the next nonlinear medium.

If the refractive index of a medium is complex then all reflection and transmission factors at input and output faces are complex (the Fresnel formulas are valid with complex refractive index). This will introduce an additional phase, depending on the value of κ_ω and $\kappa_{3\omega}$. Similarly, an additional phase will also be introduced by $\Delta\epsilon$ in Eq. (7) and by the coefficient arising from boundary conditions [Eqs. (A6)—(A8)]. This is of importance if one intends to determine the phase of nonlinear susceptibility and may modify the value of $|\chi^{(3)}|$. It can be computed exactly introducing in corresponding formulas the complex refractive index.

In our case only some liquids absorb slightly at 1.907 μm ($\kappa_\omega \sim 10^{-5}$). Thus the approximations described above are valid. Also in our special case the additional phase introduced by a complex refractive index is negligible. For example, the additional phase introduced by a reflection factor will be of the order of $\kappa_\omega/(n-1)\simeq 10^{-5}$ rad. The most significant contribution comes from $\Delta\epsilon$ and for a most drastic case (n-hexane) is equal to 0.003 rad and is also negligible.

---

[1] G. Mayer, C. R. Acad. Sci. **B267**, 54 (1968).

[2] B. F. Levine and C. G. Bethea, Appl. Phys. Lett. **24**, 445 (74); J. Chem. Phys. **65**, 2429 (1976), and references therein.

[3] J. L. Oudar, J. Chem. Phys. **67**, 446 (1977).

[4] K. D. Singer and A. F. Garito, J. Chem. Phys. **75**, 3572 (1981).

[5] I. Ledoux and J. Zyss, Chem. Phys. **73**, 203 (1982).

[6] Ch. Flytzanis, in *Quantum Electronics,* edited by H. Rabin and C. L. Tang (Academic, New York, 1975), Vol. I, p. 9.

[7] G. Hauchecorne, F. Kerhervé and G. Mayer, J. Phys. **32**, 47 (1971).

[8] J. P. Hermann, D. Ricard, and J. Ducuing, Appl. Phys. Lett. **23**, 178 (1974).

[9] J. P. Hermann, Opt. Commun. **9**, 74 (1973); **12**, 102 (1974).

[10] J. P. Hermann, thesis, Université Paris—Sud, Orsay, 1974.

[11] R. Frey and F. Pradere, Opt. Commun. **12**, 98 (1974).

[12] G. R. Meredith, B. Buchalter, and C. Hanzlik, J. Chem. Phys. **78**, 1533 (1983).

[13] G. R. Meredith, B. Buchalter, and C. Hanzlik, J. Chem. Phys. **78**, 1543 (1983).

[14] G. R. Meredith, in *Nonlinear Optical Properties of Organic and Polymeric Materials,* edited by D. J. Williams, Vol. 233 of ACS Symposium Series (American Chemical Society, Washington, D.C., 1983), p. 27.

[15] N. Bloembergen and P. S. Pershan, Phys. Rev. **128**, 606 (1962).

[16] J. Jerphagnon and S. K. Kurtz, J. Appl. Phys. **41**, 1667 (1970).

[17] S. K. Kurtz, in *Quantum Electronics,* edited by H. Rabin and C. L. Tang (Academic, New York, 1975), Vol. I, p. 209.

[18] B. F. Levine and C. G. Bethea, J. Chem. Phys. **60**, 3856 (1974).

[19] D. A. Kleinman, A. Ashkin, and G. D. Boyd, Phys. Rev. **145**, 338 (1966).

[20] J. F. Ward and G. H. C. New, Phys. Rev. **185**, 57 (1969).

[21] G. D. Boyd and D. A. Kleinman, J. Appl. Phys. **39**, 3597 (1968).

[22] *Handbook of Chemistry and Physics,* edited by R. C. Wearst and M. J. Astle (CRC Press, Boca Raton, 1982).

[23] A. J. Moses, *Optical Materials of Properties* (IFI/Plenum Data Corporation, New York, 1971), Vol. 1, p. 68.

[24] C. L. Wang and E. L. Baardsen, Phys. Rev. **185**, 1079 (1969).

[25] M. D. Levenson, IEEE J. Quantum Electron. **QE-10**, 110 (1974).

[26] A. D. Buckingham and B. J. Orr, Q. Rev. Chem. Soc. **21**, 195 (1967).

[27] *Landolt-Börnstein, Zahlenwerte und Funktionen aus Physik, Chemie, Astronomie, Geophysik, und Technik,* edited by K.-H. Hellwege and A. M. Hellwege (Springer, Berlin, 1962), Vol. II, Part 8.

[28] R. W. Hellwarth, Prog. Quantum Electron. **5**, 1 (1977).

[29] D. Chemla and P. Kupecek, Rev. Phys. Appl. **6**, 31 (1971).